

Title: The effects of graded changes in oxygen and carbon dioxide tension on coronary blood velocity independent of myocardial energy demand

Authors: Lindsey M. Boulet¹
Mike Stembridge²
Michael M. Tymko¹
Joshua C. Tremblay¹
Glen E. Foster¹

Affiliations: ¹Centre for Heart, Lung, and Vascular Health, School of Health and Exercise Science, University of British Columbia, Kelowna, Canada.
²Cardiff School of Sport, Cardiff Metropolitan University, Cardiff, UK

Correspondence: Glen E. Foster, PhD.
School of Health and Exercise Science
Faculty of Health and Social Development
University of British Columbia.
3333 University Way,
Kelowna, BC, V1V 1V7

Telephone: 250-807-8224
Fax: 250-807-9665
Email: glen.foster@ubc.ca

Running head: Coronary response to O₂ & CO₂ in humans

ABSTRACT

In humans, coronary blood flow is tightly regulated by microvessels within the myocardium in order to match myocardial energy demand. However, evidence regarding inherent sensitivity of the microvessels to changes in arterial partial pressure of carbon dioxide and oxygen is conflicting due to the accompanied changes in myocardial energy requirements. This study aimed to investigate the changes in coronary blood velocity while manipulating partial pressures of end-tidal CO₂ (P_{ET}CO₂) and O₂ (P_{ET}O₂). It was hypothesized that an increase in P_{ET}CO₂ (hypercapnia) or decrease in P_{ET}O₂ (hypoxia) would result in a significant increase in mean blood velocity in the left anterior descending artery (LAD_{Vmean}) due to an increase in both blood gases and energy demand associated with the concomitant cardiovascular response. Cardiac energy demand was assessed through non-invasive measurement of the total left ventricular mechanical energy. Healthy subjects (n=13) underwent a euoxic CO₂ test (P_{ET}CO₂ = -8, -4, 0, +4, and +8 mmHg from baseline) and an isocapnic hypoxia test (P_{ET}O₂ = 64, 52 and 45 mmHg). LAD_{Vmean} was assessed using transthoracic Doppler echocardiography. Hypercapnia evoked a 34.6 ± 8.5% (mean ± SEM; P<0.01) increase in mean LAD_{Vmean}, whereas hypoxia increased LAD_{Vmean} by 51.4 ± 8.8% (P<0.05). Multiple stepwise regressions revealed that both mechanical energy and changes in arterial blood gases are important contributors to the observed changes in LAD_{Vmean} (P<0.01). In summary, regulation of the coronary vasculature in humans is mediated by metabolic changes within the heart and an inherent sensitivity to arterial blood gases.

48 NEW & NOTEWORTHY

49 Coronary blood flow in humans is responsive to both changes in cardiac effort and arterial blood
50 gases. Using echocardiographic assessment and a non-invasively derived index of cardiac work,
51 we present an estimation of the relative contributions to coronary reactivity during CO₂ and O₂
52 challenges.

53

54 **Key words:** coronary vessels, hypoxia, carbon dioxide, echocardiography, dynamic end-tidal
55 forcing

INTRODUCTION

The coronary vasculature is capable of regulating myocardial perfusion to maintain oxygen delivery in the face of changing oxygen demands. The coronary resistance vessels can rapidly dilate in response to local tissue hypoxia thereby increasing coronary blood velocity in the major vessel branches (30, 56). Similarly, in response to increased cardiac energy demand, dilatation of coronary vessels will result in an increase in coronary blood flow to maintain oxygen delivery (59). When investigating the effect of specific stimuli on changes in coronary blood flow, it is vital to consider the stimuli's effect on cardiac energy demand. Increases in cardiac effort manifests as an increase in the rate of muscle contraction and the prevailing afterload, both increasing the overall energy expenditure and therefore coronary blood flow (2, 20, 56). The capacity of the coronary vessels to increase blood flow is often referred to as the coronary flow reserve (CFR) and can be assessed using a number of known stimuli, including alterations in arterial blood gases, such as oxygen (O_2) and carbon dioxide (CO_2). The magnitude of CFR can be used clinically as a predictor of disease states such as impaired left ventricular (LV) function, myocardial ischemia, the severity of stenosis during coronary artery disease and cardiac mortality (14, 31, 33). In addition, CFR can guide clinical decisions regarding patient revascularization (8). Assessing CFR in a clinical population typically involves invasive catheterization and the administration of a pharmacological agent; this study aims to demonstrate the utility of a non-invasive and pharmacological-free assessment of CFR using echocardiography and blood gas control techniques.

Carbon dioxide has long been implicated as a regulator of the coronary arteries in both animal studies and isolated preparations (9). Such studies have correlated an increase in myocardial blood flow with increasing partial pressure of CO_2 (PCO_2) in the coronary sinus (3,

26). A complementary effect was observed in follow-up studies suggesting that a decrease of PCO_2 in the coronary circulation results in an observable decrease in blood flow (3, 6, 50), which has been demonstrated using coronary sinus catheterization in both healthy subjects (36) and those with a stable cardiac disorder (21, 32, 35). Myocardial oxygen consumption (MVO_2) was measured in two of these studies and found that hypocapnia had no significant effect on overall cardiac energy demand (21, 32). These hypercapnic and hypocapnic effects have been repeated in human studies using MRI (4, 54) PET imaging (55) and echocardiography (49); all of which reported the same results as the previous invasive studies. However, some studies involving hypercapnia show either no change in MVO_2 (54) or no change in coronary blood flow after normalizing for the increase in MVO_2 (55), suggesting the inherent sensitivity of the coronary vasculature to changes in PCO_2 remains to be determined.

The limited oxygen extraction reserve of the myocardial tissue paired with an equally limited ability to perform anaerobic respiration causes the heart to rely heavily on changes in coronary blood flow to match MVO_2 (56). MVO_2 is tightly linked to cardiac work and is the main stimulus for changes in coronary blood flow; this recognition led to the development of cardiac work indices in an effort to accurately evaluate coronary reactivity non-invasively (18). RPP is a product of HR and systolic pressure, it was the first index developed and it was adopted in clinical settings due to the simplicity of the measurements involved (18). RPP is still commonly used in coronary vascular studies though it neglects important factors that contribute to MVO_2 such as myocardial elastic potential energy and external work (41). Recently, an index of LV function has been developed using a non-invasive estimation of myocardial elastance that allows an investigator to assess the elastic potential energy of the heart (7). This index is well correlated with invasive measures of myocardial contractility and has been adopted for clinical

102 assessments of LV function (38, 40, 52). Along with non-invasive left ventricular pressure and
103 volume estimations, it can be used to generate non-invasive pressure volume relationships, which
104 might provide a less variable index of total mechanical energy than RPP. This was the first
105 coronary blood flow study to use this non-invasively derived pressure volume loop as an
106 estimate of cardiac effort.

107 The purpose of this study was to observe the direct effects of acute isocapnic hypoxia,
108 euoxic hypocapnia, and euoxic hypercapnia, on coronary blood velocity in humans. As well as to
109 quantify the changes in cardiac energy demand as a surrogate for MVO_2 to determine whether
110 the sensitivity of the coronary vasculature to PO_2 and PCO_2 is a product of increased cardiac
111 effort associated with the stimulus itself. It was hypothesized that coronary blood flow would
112 increase from baseline during hypoxia and hypercapnia and that it would decrease during
113 hypocapnia. Secondly, it was hypothesized that cardiac effort would increase during the hypoxic
114 and hypercapnic interventions, and cardiac effort would be the primary contributor to increases
115 in coronary blood velocity.

116 **METHODS**

117 **Ethical Approval**

118 All experimental procedures and protocols were submitted to and approved by the Clinical
119 Research Ethics Board at the University of British Columbia and conformed to the Canadian
120 Government Tri-Council Policy Statement on research ethics (TCPS2). All participants provided
121 written informed consent prior to participation in this study.

122 **Participants**

123 All experiments were conducted in the cardiopulmonary laboratory for experimental and applied
124 physiology (Kelowna, BC). Twenty-two male participants were recruited for the current study;
125 eight of these participants were excluded due to an inability to adequately visualize the LAD
126 using color Doppler imaging, through the participant's intercostal acoustic windows. To avoid
127 the known potential sex differences when assessing coronary reactivity, this study included only
128 male participants (22). One participant was excluded for having a resting coronary velocity that
129 exceeded two standard deviations above the group mean. Participants were excluded if they
130 were obese (body mass index $\geq 30 \text{ kg m}^{-2}$), had a history of smoking, were hypertensive (systolic
131 blood pressure $> 140 \text{ mmHg}$; diastolic blood pressure $> 90 \text{ mmHg}$), were on medication or had
132 poor pulmonary function as determined by spirometry (ratio of forced expiratory volume in 1s to
133 forced vital capacity $< 75\%$ of predicted). Participants included in the mean analysis were
134 healthy males ($n = 13$) with no history of cardiovascular, pulmonary or neurological disease.

135 **Experimental Protocol**

136 Participants visited the lab on two separate occasions. On the first visit the participants' height
137 and weight was recorded and spirometry was performed in accordance with the standards set

forth by the American Thoracic Society and the European Respiratory Society joint guidelines (28). The participants were also screened using echocardiography to ensure that coronary artery velocity was measureable. Finally, participants were asked to fill out a questionnaire to ensure they met the inclusion criteria (above).

Upon arrival for the second visit, participants were instrumented with an electrocardiogram in lead-II configuration, connected to a bio amp (FE132, ADI Instruments, Colorado Springs, CO, USA) to measure instantaneous heart rate (HR). A pulse oximeter (ML320/F, ADI Instruments) was placed on the right index finger to measure arterial oxyhemoglobin saturation (SpO_2). Beat-by-beat systolic (SBP), diastolic (DBP), and mean arterial pressure (MAP) was measured from a cuff placed on the mid-phalanx of the right middle finger using finger pulse photoplethysmography (Finometer PRO; Finapres Medical Systems, Amsterdam, the Netherlands). Return-to-flow calibration was performed prior to every trial in order to calibrate blood pressure to a reconstructed brachial artery waveform (15). The participants wore a nose clamp and breathed through a mouthpiece, bacteriological filter, and a two-way non-rebreathing valve (2600 series, Hans Rudolph, Shawnee, KS, USA). Electrocardiogram, blood pressure, respiratory flow and respired gases (O_2 and CO_2) were acquired at 200 Hz using an analog-to-digital converter (Powerlab/16SP ML 880; ADInstruments) interfaced with a personal computer and analyzed with commercially available software (LabChart V7.1, ADInstruments). Respiratory flow was measured near the mouth using a pneumotachograph (HR 800L, HansRudolph) and a differential pressure transducer (1110 series, HansRudolph), which was zeroed and calibrated using a 3-liter syringe before experimentation. Minute ventilation (\dot{V}_E) was calculated as a product of i) tidal volume (V_T), which was determined using an integral of the respiratory flow signal, and ii) breathing

frequency (F_B), defined as the number of breaths per minute. Respired gas partial pressures were sampled near the mouth, dried with nafion tubing in desiccant, and analyzed for end-tidal PO_2 ($P_{ET}O_2$) and PCO_2 ($P_{ET}CO_2$) (ML206, ADinstruments). Gas analyzers were calibrated before and verified following each protocol using a calibration gas with known concentrations of CO_2 and O_2 . Time corrections were applied to the PO_2 and PCO_2 signal to account for the gas analyzer delay and values corresponding to the moment of end expiration were identified as the $P_{ET}O_2$ and $P_{ET}CO_2$. A dynamic end-tidal forcing system was used to clamp and manipulate both $P_{ET}O_2$ and $P_{ET}CO_2$ throughout the protocol as previously described (44, 47, 48). After instrumentation, a normoxic CO_2 reactivity test was conducted first, followed by a 30-minute rest and an isocapnic hypoxia reactivity test in succession; the trials were not randomized in order to avoid any carryover effects of hypoxia on sympathetic nervous system activation (53).

Normoxic CO_2 Reactivity. Following instrumentation, participants breathed room air while baseline $P_{ET}CO_2$, $P_{ET}O_2$ and echocardiographic measurements were recorded. Immediately following baseline, $P_{ET}CO_2$ was reduced through active hyperventilation to -8 and -4 mmHg from baseline, after the hypocapnic steps, $P_{ET}CO_2$ was allowed to return to baseline values. The hypercapnic protocol was then initiated, where the participants' $P_{ET}CO_2$ was increased to +4 and +8 mmHg using the end tidal forcing system that continually adjusts CO_2 delivery on a breath-by-breath basis in response to target the desired end tidal values. Each stage lasted for approximately 8 minutes. Throughout the protocol $P_{ET}O_2$ was maintained at normoxic levels. The collection of echocardiographic images began following two minutes of stable end-tidal gases. This protocol was selected because it permitted the assessment of coronary blood velocity throughout the hypo- and hyper-capnia range.

Isocapnic Hypoxia Reactivity. During an initial ten-minute baseline period, resting $P_{ET}O_2$, $P_{ET}CO_2$ and echocardiography measurements were collected. Next, $P_{ET}O_2$ was reduced using the end tidal forcing system that delivers air with a low fraction of O_2 on a breath-by-breath basis in response to target desired end tidal values. The system held $P_{ET}O_2$ at three stages of acute hypoxia (64, 52, 45 mmHg) that lasted 8 minutes, while maintaining isocapnia. Echocardiographic images were collected at each stage following two minutes of stable end-tidal gases. This protocol was selected because it permitted the assessment of coronary blood velocity through the hypoxic range and across a linear change in SpO_2 (37).

Measurements

Echocardiography. All echocardiographic measurements were collected on a commercially available ultrasound system (Vivid E9, GE, Fairfield, CT, USA) using a broadband M5S 5 MHz or a 3V 3D-array transducer. The same trained sonographer collected all the images for the study; the sonographer has previously published test-retest reliability data for structural cardiac measurements (39). The sonographer's reliability in measuring LAD_V were measured in this study and were statistically analyzed using the Cronbach's alpha reliability test intended to determine the correlation of two separate interrogations of the same construct. Based on a sample size of 14, the alpha values were found to be 0.81 and 0.89 for the max and mean velocities respectively, suggesting good consistency between measurements. Images were captured and saved for offline analysis using commercially available software (EchoPAC v.13, GE). All echocardiographic values represent an average value of three cardiac cycles representing the clearest of five collected images for each experimental stage. Echocardiographic measurements are described in detail below. Following instrumentation, the collapsibility index of the inferior vena cava (IVC) was assessed during inspiration as previously

described (36) and used to estimate right atrial pressure. An IVC, with an initial diameter \leq 2.1cm, that collapses more than 50% are assumed to have a normal right atrial pressure of 3 mmHg. Participants were then moved to a left lateral decubitus position for the collection of the remaining measurements.

Coronary Blood Velocity. Left anterior descending (LAD) coronary artery blood velocity (LAD_v) was measured from the distal section of the LAD using previously described echocardiographic techniques (19, 23, 49). LAD_v measurements made by transthoracic echocardiography have been previously shown to closely correlate with intracoronary Doppler guide wire measurements (24). LAD_v measurements were obtained during the last minute of baseline and each stage of the normoxic CO₂ reactivity test and the isocapnic hypoxia reactivity test. The LAD was imaged using a modified parasternal short axis view from the fourth or fifth left intercostal space and was assessed using pulsed-wave Doppler. The transducer was positioned such that a 2-3 mm segment of the LAD was imaged along the long-axis taking care to align the pulse-wave cursor with the length of the vessel. With a sample volume (2.0 mm) positioned over the color Doppler signal in the LAD, measurements of the LAD_v were collected during a short end-expiratory apnea. The collected waveforms were analyzed to determine mean diastolic velocity (LAD_{vmean}) and peak diastolic velocity (LAD_{vmax}) (Fig. 1). For each stage, the average value for three cardiac cycles is reported. Coronary vascular resistance (CVR) was estimated as MAP/LAD_{vmean} .

Pulmonary and Cardiac Hemodynamics. 3D triplane assessment of the left ventricle was used to obtain volume measurements; using a 3D-array transducer three two dimensional apical images were simultaneously obtained, 60° adjacent to each other, representing a standard four, three, and two chamber view. The images are then transferred to an offline workstation and

analyzed by a trained investigator. By manually tracking the endocardial border of each image with the analysis software it was possible to estimate the longitudinal geometry of the left ventricle at three adjacent axes from one heart beat. Using the three measurements from the 2D images, the analysis software is able to estimate the end systolic and diastolic volumes by assuming a relatively circular cross-sectional area of the ventricle, similar to the Simpson's biplane method (42). Data was collected from three heartbeats during each condition and averaged to produce one value.

Left Ventricular Energy Demand. Two indices were used in this study in an effort to account for the change in myocardial energy demand and its influence on coronary blood flow. First, the minute mechanical energy of the left ventricle (ME_{LV}) was estimated using a non-invasive method (7) and second, the rate-pressure product (RPP) was calculated. ME_{LV} was calculated using a non-invasive pressure-volume loop and a validated estimate of LV elastance (E_{Nd}) (7). Stroke work is defined as the area within a pressure-volume loop and, assuming that the end-diastolic pressure volume relationship is negligible and constant across experimental conditions, it can be estimated noninvasively by plotting end systolic volume (ESV), end diastolic volume (EDV), SBP and DBP for each condition (7, 44). E_{Nd} was estimated using a model developed from a group-averaged normalized elastance curve value derived from the data of 23 separate studies that employed invasive measurement techniques to obtain LV and aortic pressure-volume relationships (7). Individual elastance values for each subject were estimated and corrected for EF, the ratio of DBP to SBP and the time ratio of the isovolumic contraction period to the total systolic period (7). The isovolumic contraction period and total systolic period can be identified through a Doppler investigation of the aortic outflow in a five-chamber view time aligned to an ECG signal. Potential energy was estimated by plotting E_{Nd} tangentially to the end systolic point

with the area under the slope representing elastic potential energy (Fig. 2). The area under the pressure volume curve represents the energy expended by the heart in one cardiac cycle (PV_A) in $ml \cdot mmHg$ which is then converted to Joules by applying a conversion factor of 1.3×10^{-4} . Multiplying the calculated energy by HR produces the rate of total LV mechanical energy generated (ME_{LV} ; J/min) (7). RPP was calculated as the product of the average HR and SBP for each experimental stage (18).

Statistical Analysis

Statistical comparisons and calculations were conducted in R (<http://cran.r-project.org/>). LAD_v metrics, pulmonary and cardiac hemodynamics and LV work parameters were all compared between each experimental PCO_2 and PO_2 stage using a one-way analysis of variance (ANOVA) with repeated measures. In order to determine the contribution of cardiac work and perfusion pressure on changes in LAD_{vmean} , an analysis of covariance (ANCOVA) was used to examine changes in LAD_{vmean} between the experimental stages while using ME_{LV} and MAP as covariates. Tukey's HSD test was applied to all analyses with significant F-ratios to determine which conditions were significantly different. Multiple stepwise regressions were used to determine which variables contribute to the observed changes in LAD_{vmean} in both CO_2 and O_2 reactivity protocols. The following independent variables were included in the regression equation: SpO_2 , $P_{ET}CO_2$, MAP, SBP, DBP, RPP and ME_{LV} . The tolerance to determine the inclusion criteria of an independent variable in the regression model was set at $P < 0.05$. Standardized beta weights were then applied to determine the predictive value of the selected independent variables. The Pearson's product-moment was used to correlate LAD_{vmean} to both ME_{LV} and RPP as well as to correlate RPP to ME_{LV} . Individual coronary blood velocity reactivity's were calculated as the slope of the linear regression for all three interventions (i.e. hypocapnia, hypercapnia and

275 hypoxia) by regressing $LAD_{V_{mean}}$ with either SpO_2 or $P_{ET}CO_2$. All data was presented as mean \pm
276 SEM and statistical significance was set at $P < 0.05$ for all comparisons.

RESULTS

Participants.

Participants included (n=13) in the hypercapnic and hypoxic trials had a mean \pm SEM age of 25.5 ± 1.4 years, weight of 78.3 ± 2.4 kg, height of 179.8 ± 1.6 cm, and a BMI of 24.2 ± 0.5 kg/m². Participants were normotensive (systolic blood pressure = 117 ± 5 mmHg, diastolic blood pressure = 64 ± 3 mmHg) and had a resting heart rate of 55 ± 2 bpm. Subjects had healthy lung function with an average FEV₁ of 4.65 ± 0.72 L ($99 \pm 2.7\%$ of predicted values) and an FEV₁/FVC ratio that was $99.8 \pm 1.5\%$ of predicted values.

Protocol 1: Euoxic Hypocapnia and Hypercapnia.

Table 1 demonstrates the cardiovascular and hemodynamic variables during each stage of hypo- and hyper-capnia. P_{ET}CO₂ was well controlled during both hypercapnic and hypocapnic stages and SpO₂ was constant throughout the protocol ($P > 0.9$). LAD_{Vmax} increased significantly above baseline during the +8 mmHg hypercapnic stage ($P < 0.01$), though did not change during hypocapnia ($P > 0.99$). Figure 1 demonstrates representative traces of coronary velocity at baseline and during hypercapnia. Both SBP and DBP were significantly elevated during both hypercapnic stages ($P < 0.02$). There was a tendency for HR to increase during hypercapnia but it did not reach significance ($P > 0.06$). EDV and ESV did not change from baseline during either the hypercapnic and hypocapnic exposure ($P = 0.99$). RPP increased $26.8 \pm 7.2\%$ and $41.3 \pm 6.5\%$ above baseline with increasing hypercapnia ($P = 0.05$) and did not change during the hypocapnic stages ($P = 0.64$). PV_A displayed an increasing trend through the hypercapnic trials, though did not reach significance ($P = 0.07$). Figure 3 shows the LAD_{Vmean}, MAP, CVR, ME_{LV}, and LAD_{Vmean} as a function of ME_{LV} (i.e. LAD_{Vmean}/ME_{LV}) across the hypocapnic and hypercapnic range. ME_{LV} showed a significant increase ($P = 0.02$) above baseline by 27.9 ± 6.1

% and $42.8 \pm 6.5\%$, corresponding to the increasing levels of CO_2 , with no change during hypocapnia ($P = 0.61$) (Fig. 3). MAP increased above baseline values during mild and moderate hypercapnic exposure ($P < 0.01$) and was unaltered by hypocapnia ($P = 0.3$). CVR did not significantly change from baseline ($P = 0.57$). Mild and moderate hypercapnia (i.e. $P_{\text{ETCO}_2} = +4, +8$ mmHg from baseline) induced significant increases in $\text{LAD}_{\text{Vmean}}$ from baseline. During hypocapnia, there was no significant change in $\text{LAD}_{\text{Vmean}}$ ($P > 0.99$). When indexed against total ME_{LV} , $\text{LAD}_{\text{Vmean}}$ remained unchanged from baseline. Figure 4 displays the individual and mean coronary reactivity in the hypocapnic and hypercapnic range. Mean coronary reactivity was found to be 0.13 ± 0.13 cm/s/mmHg during hypocapnia and 0.95 ± 0.11 cm/s/mmHg during hypercapnia.

Evaluating the change in $\text{LAD}_{\text{Vmean}}$ in response to changes in P_{ETCO_2} shows no significant effect when using ME_{LV} or RPP as a covariate ($P = 0.24$; $P = 0.34$). Correlating $\text{LAD}_{\text{Vmean}}$ to ME_{LV} and RPP using the Pearson's product-moment correlation revealed an r-value of 0.57 and 0.55 respectively ($P < 0.01$). ME_{LV} and RPP were also found to be correlated with an r-value of 0.64 ($P < 0.01$). Changes in ME_{LV} ($P < 0.01$) and P_{ETCO_2} ($P < 0.01$) were identified as the major contributors to changes in $\text{LAD}_{\text{Vmean}}$ through multiple stepwise regression analysis. Multiple linear regression analysis indicates that 36% of the $\text{LAD}_{\text{Vmean}}$ response is related to changes in P_{ETCO_2} while 44% of the $\text{LAD}_{\text{Vmean}}$ response is related to changes in ME_{LV} ($R = 0.66$; $P < 0.01$).

Protocol 2: Isocapnic Hypoxia

321 Table 2 demonstrates the cardiovascular and hemodynamic variables at baseline and during each
 322 stage of hypoxia. $P_{ET}O_2$ and consequently SpO_2 were well controlled during the three stages of
 323 hypoxia, whereas $P_{ET}CO_2$ was held constant throughout the protocol ($P > 0.9$). LAD_{Vmax} was
 324 elevated above baseline during both the 52 mmHg and 45 mmHg stages of hypoxia ($P < 0.01$).
 325 Systolic blood pressure increased significantly during the 45 mmHg $P_{ET}O_2$ stage while diastolic
 326 blood pressure tended to increase, but was not statistically significant ($P < 0.01$; $P = 0.07$). Both
 327 the 52 and 45 mmHg $P_{ET}O_2$ stages caused elevations in HR from baseline by $19.7 \pm 4.2\%$ ($P =$
 328 0.02) and $29.8 \pm 5.7\%$ ($P < 0.01$) respectively. EDV and ESV did not change from baseline
 329 during the hypoxic exposure ($P = 0.99$). RPP was elevated by $30.2 \pm 5.0\%$ and $48.3 \pm 7.8\%$ ($P <$
 330 0.01) during the 52 and 45 mmHg $P_{ET}O_2$ stages, respectively. PV_A was not significantly
 331 elevated during any of the hypoxic trials ($P = 0.4$). Figure 5 shows the LAD_{Vmean} , MAP, CVR,
 332 ME_{LV} , and LAD_{Vmean} as a function of ME_{LV} (i.e. LAD_{Vmean}/ME_{LV}) during baseline and across the
 333 three stages of hypoxia. ME_{LV} was elevated from baseline during the 52 and 45 mmHg $P_{ET}O_2$
 334 stages of hypoxia ($P < 0.01$). MAP was elevated from baseline during the 45 mmHg $P_{ET}O_2$ stage
 335 ($P = 0.02$). CVR decreased significantly from baseline during the 45 mmHg $P_{ET}O_2$ stage ($P =$
 336 0.02). Both the 52 and 45 mmHg $P_{ET}O_2$ stages resulted in a significant increase in LAD_{Vmean} (P
 337 < 0.01). When indexed against ME_{LV} , LAD_{Vmean} did not significantly change from baseline.
 338 Mean coronary reactivity was found to be 0.74 ± 0.09 cm/s/%desaturation during hypoxia (Fig.
 339 6).

340 Evaluating the changes in LAD_{Vmean} due to decreasing SpO_2 shows no change when using ME_{LV}
 341 or RPP as a covariate ($P = 0.67$; 0.26). Pearson's product-moment correlation determined an r
 342 value of 0.66 and 0.55 when correlating LAD_{Vmean} to ME_{LV} and RPP respectively ($P < 0.01$).
 343 Correlating RPP to ME_{LV} produced an r-value of 0.71 ($P < 0.01$). Using multiple stepwise

344 regressions analysis, it was determined that changes in ME_{LV} ($P < 0.01$) and SpO_2 ($P < 0.01$)
345 were the major contributors to increases in LAD_{Vmean} . Multiple linear regression analysis implies
346 that 38% of the LAD_{Vmean} response is related to changes in SpO_2 while 45% of the LAD_{Vmean}
347 response is related to changes in ME_{LV} ($R = 0.73$; $P < 0.01$). It is important to note that all of the
348 analyses were completed using LAD_{Vmean} as the outcome variable, though a similar result is
349 found using LAD_{Vmax} (see tables 1 & 2).

DISCUSSION

This is the first study to quantify the changes in LAD_v in young, healthy humans exposed to euoxic hypo- and hyper-capnia, and isocapnic hypoxia while non-invasively estimating total left ventricular mechanical energy. The main findings of this study suggest that i) exposure to hypercapnia (+4, +8 mmHg) significantly elevates both $LAD_{V_{mean}}$ and ME_{LV} while hypocapnia did not, ii) hypoxia (52, 45 mmHg $P_{ET}O_2$ stages) elicits an increase in both $LAD_{V_{mean}}$ and ME_{LV} , and iii) the sensitivity of the LAD to hypercapnia and hypoxia in humans is the combination of the inherent vascular sensitivity to CO_2 and O_2 , and the increase in total mechanical energy due to the cardiovascular responses associated with each stressor.

Response to Carbon Dioxide

A small number of studies have assessed the effects of hypercapnia on the coronary vasculature in humans and although it is generally accepted that an increase in blood flow occurs, there is not yet agreement on the specific contributions of vessel sensitivity to CO_2 and the associated increase in MVO_2 . The current study found increases in absolute LAD_v in response to hypercapnia, which is consistent with previous studies in both healthy and clinical populations (4, 21, 49, 55). An observed increase in cardiac effort, represented by ME_{LV} and RPP, suggests that vessel sensitivity to CO_2 is not the sole stimulus for the observed increase in $LAD_{V_{mean}}$. Previous reports have suggested that there is no change in coronary blood flow in response to hypercapnia when controlling for cardiac effort (55). The accepted conclusion drawn by most animal and human studies is that the sensitivity of the coronary vasculature to hypercapnia is orders of magnitudes less than its sensitivity to hypercapnic-induced increases in cardiac work (10, 34, 55). Using ME_{LV} or RPP as index of work and calculating the change in the ratio of work to changes in $LAD_{V_{mean}}$ yielded no significant change in velocity, similar to previous work.

However, there is previous evidence of a coronary response to hypercapnia with no change in cardiac effort while using direct measurements of MVO_2 , suggesting that non-invasive methods used to correct for the change in cardiac energy demand may not be valid (3, 21). Indeed, the correlations between $\text{LAD}_{\text{Vmean}}$ and RPP or ME_{LV} resulted in relatively weak relationships ($r = 0.55; 0.66$), inferring the need for a more detailed analysis to determine the exact individual contributions of cardiac effort and changes in P_{ETCO_2} . Likewise, the relationship between RPP and ME_{LV} can only account for some of the variability between two variables meant to serve as a surrogate for the same parameter (i.e. MVO_2). Multiple stepwise regression analysis determined that of all the implicated variables (SpO_2 , P_{ETCO_2} , MAP, SBP, DBP, RPP and ME_{LV}), ME_{LV} and P_{ETCO_2} are the only significant predictors of changes in $\text{LAD}_{\text{Vmean}}$. Using standardized beta weights, it also determined that the contributions of P_{ETCO_2} ($\beta = 0.36$) are relatively comparable to those of ME_{LV} ($\beta = 0.44$), contrary to previous reports. When compared to the cerebrovascular bed, absolute coronary reactivity was found to be of a similar magnitude ($\sim 4\text{--}5\%/ \text{mmHg}$) (1, 4). Though considering the fact that 44% of the hypercapnic reactivity is due to increased cardiac effort, it can be surmised that the cerebrovasculature is more sensitive to hypercapnia than the coronary circuit. The brachial artery has been found to be less sensitive to hypercapnia than cerebral vessels. However, when comparing relative reactivity, our results as well as other published results suggest that the coronary vessels are the least sensitive of the three (51).

Hypocapnia did not elicit any significant changes in any hemodynamic or cardiovascular variables. Most hypocapnic human studies have determined that a decrease in arterial partial pressure of CO_2 through voluntary or mechanical hyperventilation results in a corresponding decrease in coronary blood flow in both healthy subjects and those with coronary artery disease

or a cardiac disorder (21, 33, 35). MVO_2 remains unchanged during the hypocapnic exposure in these investigations, implicating the involvement of another mechanism in the control of coronary blood flow outside of myocardial energy expenditure (21, 32). The leftward shift of the oxyhemoglobin dissociation curve during alkalosis leading to an increase in oxygen extraction could offer an explanation for the observed decrease in coronary flow during hypocapnia previously observed (21, 35). Similar to previous work we found no significant change in cardiac effort; however, in contrast we observed no change in $\text{LAD}_{\text{Vmean}}$ during hypocapnia. The duration of exposure to hypocapnia (21) or the magnitude of hypocapnia (32) may explain this discrepancy between studies.

Response to Hypoxia

Few studies have characterized the vasodilatory effects of hypoxia on the human coronary circulation; those that have are in agreement with animal studies. Similar to previous work, this study found a significant increase in $\text{LAD}_{\text{Vmean}}$ (4, 29). Hypoxia causes a dissociation reaction in oxyhemoglobin that ultimately results in the release of ATP into the vessel lumen; it, along with its metabolites (ADP, AMP, Adenosine) activate endothelial adenosine receptors which result in smooth muscle relaxation and ultimately vessel dilation (11). This hypoxic mechanism can occur via systemic hypoxia or cardiac workload induced hypoxemia; for this reason, during an experimental hypoxic challenge, it is particularly difficult to demarcate the specific contributions of cardiac effort and the applied hypoxia (45, 46). Regardless, using an index of cardiac effort, human investigations have determined that hypoxia causes a significant increase in coronary flow above and beyond the changes in cardiac effort (4, 29). Investigations aimed at correlating coronary reactivity to cerebrovascular reactivity during hypoxia have found a similar response to decreased arterial partial pressure of O_2 in both circulations when coronary reactivity is

normalized to cardiac work (4). Compared to the previous human studies that did not report any changes in the cardiovascular or hemodynamic variables, our study found increases in SBP, MAP and HR during hypoxia. Considering these studies report a significant increase in RPP, it can be surmised that an increasing trend in HR, MAP and SBP was likely observed during hypoxia. The results presented here determine that an increase in cardiac effort, estimated by both ME_{LV} and RPP, occurs during hypoxia and that indexing either RPP or ME_{LV} to LAD_{Vmean} results in no significant change with increasing hypoxia. Similar to the hypercapnic trials, a weak correlation is found between LAD_{Vmean} and RPP or ME_{LV} ($r = 0.55$; 0.66) suggesting that using a ratio of LAD_{Vmean} to either measure of cardiac effort might be an over simplified solution. Stepwise multiple regressions of all possible contributors (SpO_2 , P_{ETCO_2} , MAP, SBP, DBP, RPP and ME_{LV}) to changes in LAD_{Vmean} determined that SpO_2 and ME_{LV} were the only significant predictors. Calculating standardized units, it was determined that SpO_2 and ME_{LV} were relatively equal predictors for changes in LAD_{Vmean} at approximately 38% and 45% respectively. This information implies that ME_{LV} is likely a more sensitive estimate of cardiac effort than RPP and that blood pressure which contributes by both influencing cardiac afterload and coronary perfusion pressure does not appear to improve the model more than ME_{LV} alone. Based on previous reports and the data from this study, the cerebral and brachial circulation have a larger reactivity to hypoxia ($\sim 1.3\%/ \%SpO_2$; $\sim 1.5\%/ \%SpO_2$ respectively) than the coronary vessels ($\sim 0.7\%/ \%SpO_2$) (25, 27).

Limitations

Doppler investigation of the coronary artery acts as a useful index of actual blood flow. However, B-mode images of the vessel itself lack the spatial resolution to measure the diameter. It is therefore not possible to directly quantify flow through our transthoracic ultrasound

approach. However, it has been demonstrated that the majority of vessel dilation occurs in the downstream microvessels and Doppler investigation of coronary blood velocity has been shown to be highly correlated to actual coronary flow (17, 56). Recently, measurements of coronary blood velocity at baseline and during isocapnic hypoxia ($P_{ET}O_2 = 45$ mmHg) were made in healthy participants and cross-sectional area of the LAD was acquired in three subjects using cardiac MRI (13). $LAD_{V_{mean}}$ was similar between imaging modalities and the cross-sectional area at baseline (22.3 ± 4.5 mm²) did not differ from hypoxia (22.4 ± 5.3 mm²). These data, albeit, in a small subset of healthy humans suggests that our measures of LAD_v are reflective of blood flow due to downstream microvessel dilation. To ensure the Doppler measure was accurately estimating blood velocity, effort was made to align the long axis of the vessel with the pulse wave cursor.

The non-invasive pressure-volume loop used to calculate ME_{LV} requires the assumption that the end diastolic pressure volume relationship (EDPVR) is equal to zero. Though untrue, it is a reasonable assumption for two reasons: (1) the study was designed for within subject comparisons which effectively nullifies any differences in actual EDPVR between subjects and (2) it is unlikely that, during either protocol, the compliance of the myocardium was altered significantly, therefore there should not be any variability in EDPVR within subject. A further limitation of the non-invasively pressure-volume loop regards the use of a reconstructed blood pressure waveform from the finger as an estimate of systolic and diastolic left ventricular pressures. All non-invasive estimations of cardiac workload are associated with assumptions, though it is undoubtedly an important consideration for evaluating LV function in both clinical and research settings. Simple indices such as RPP or the pressure work index offer quick estimations of cardiac effort using easily obtained measurements (HR, SBP, DBP), but their

derivations lack certain variables that contribute to total cardiac effort (18). ME_{LV} employs certain important components of cardiac effort such as left ventricular end-systolic elastance and measured ventricular volumes. As demonstrated here RPP follows a similar trend in response to stimuli as ME_{LV} though they are weakly correlated during hypercapnia and hypoxia ($r = 0.64$; 0.71). Further stepwise regression analysis demonstrated the increased sensitivity of ME_{LV} in predicting the observed changes in coronary blood flow, which suggests that using a comprehensive non-invasive index of cardiac effort that includes multiple parameters can offer more insight into cardiac work.

In conclusion this study demonstrated that coronary blood flow is influenced nearly equally by both arterial blood gases and the associated changes in cardiac effort during hypercapnia and hypoxia. This is a novel finding considering that to date, the majority of investigations of human coronary vascular response to hypercapnia and hypoxia have concluded that the changes in coronary flow are solely due to the increases in cardiac work and not the manipulations of arterial blood gases. Furthermore, it was demonstrated that ME_{LV} is a more accurate estimate of cardiac effort than RPP, which is far more commonly used. Considering the profound effect cardiac workload has on coronary blood flow, using an index that includes more information regarding the mechanical parameters of the heart could improve precision when measuring coronary vessel sensitivity. Given the previously observed sex differences in coronary reactivity, future directions would aim to extend this work to quantify and compare the response differences between males and females.

485 **ACKNOWLEDGEMENTS**

486 We are grateful to our subjects volunteering their time to complete this study.

487 **GRANTS**

488 Natural Sciences and Engineering Research Council of Canada and Canada Foundation for
489 Innovation

490 **DISCLOSURES**

491 None

492

493 **REFERENCES**

- 494 1. **Ainslie PN, Murrell C, Peebles K, Swart M, Skinner MA, Williams MJ and Taylor RD.**
495 Early morning impairment in cerebral autoregulation and cerebrovascular CO₂ reactivity in
496 healthy humans: relation to endothelial function. *Exp Physiol* 92: 4: 769-777, 2007.
- 497 2. **Alders DJ, Groeneveld AB, de Kanter FJ and van Beek JH.** Myocardial O₂ consumption in
498 porcine left ventricle is heterogeneously distributed in parallel to heterogeneous O₂ delivery. *Am*
499 *J Physiol Heart Circ Physiol* 287: 3: H1353-H1361, 2004.
- 500 3. **Alexander CS and Liu SM.** Effect of hypercapnia and hypocapnia on myocardial blood flow
501 and performance in anaesthetized dogs. *Cardiovasc Res* 10: 3: 341-348, 1976.
- 502 4. **Beaudin AE, Brugniaux JV, Vohringer M, Flewitt J, Green JD, Friedrich MG and**
503 **Poulin MJ.** Cerebral and myocardial blood flow responses to hypercapnia and hypoxia in
504 humans. *Am J Physiol Heart Circ Physiol* 301: 4: H1678-H1686, 2011.
- 505 5. **Berne RM, Blackmon JR and Gardner TH.** Hypoxemia and coronary blood flow. *J Clin*
506 *Invest* 36: 7: 1101-1106, 1957.
- 507 6. **Case RB, Greenberg H and Moskowitz R.** Alterations in coronary sinus pO₂ and O₂
508 saturation resulting from pCO₂ changes. *Cardiovasc Res* 9: 2: 167-177, 1975.
- 509 7. **Chen CH, Fetters B, Nevo E, Rochitte CE, Chiou KR, Ding PA, Kawaguchi M and Kass**
510 **DA.** Noninvasive single-beat determination of left ventricular end-systolic elastance in humans.
511 *J Am Coll Cardiol* 38: 7: 2028-2034, 2001.

- 512 8. **Courtis J, Rodes-Cabau J, Larose E, Potvin JM, Dery JP, Larochelliere RD, Cote M,**
513 **Cousterousse O, Nguyen CM, Proulx G, Rinfret S and Bertrand OF.** Usefulness of coronary
514 fractional flow reserve measurements in guiding clinical decisions in intermediate or equivocal
515 left main coronary stenoses. *Am J Cardiol* 103: 7: 943-949, 2009.
- 516 9. **Crystal GJ.** Carbon Dioxide and the Heart: Physiology and Clinical Implications. *Anesth*
517 *Analg* 121: 3: 610-623, 2015.
- 518 10. **Daugherty JRM, Scott JB, Dabney JM and Haddy FJ.** Local effects of O₂ and CO₂ on
519 limb, renal, and coronary vascular resistances. *Am J Physiol* 213: 5: 1102-1110, 1967.
- 520 11. **Deussen A, Brand M, Pexa A and Weichsel J.** Metabolic coronary flow regulation--current
521 concepts. *Basic Res Cardiol* 101: 6: 453-464, 2006.
- 522 12. **Feigl EO.** Coronary physiology. *Physiol Rev* 63: 1: 1-205, 1983.
- 523 13. **Foster GE, Deng Z, Boulet LM, Mehta PK, Wei J, Fan Z, Dharmakumar R, Merz CNB,**
524 **Li D and Nelson MD.** Changes in left ventricular function and coronary blood flow velocity
525 during isocapnic hypoxia: A cardiac magnetic resonance imaging study. *J Cardiovasc Magn*
526 *Reson* 18: 2016.
- 527 14. **Gould KL, Kirkeeide RL and Buchi M.** Coronary flow reserve as a physiologic measure of
528 stenosis severity. *J Am Coll Cardiol* 15: 2: 459-474, 1990.
- 529 15. **Guelen I, Westerhof BE, Van Der Sar GL, Van Montfrans GA, Kiemeneij F, Wesseling**
530 **KH and Bos WJ.** Finometer, finger pressure measurements with the possibility to reconstruct
531 brachial pressure. *Blood Press Monit* 8: 1: 27-30, 2003.

- 532 16. **Hilton R and Eichholtz F.** The influence of chemical factors on the coronary circulation.
533 *Am J Physiol* 59: 6: 413-425, 1925.
- 534 17. **Hirata K, Amudha K, Elina R, Hozumi T, Yoshikawa J, Homma S and Lang CC.**
535 Measurement of coronary vasomotor function: getting to the heart of the matter in cardiovascular
536 research. *Clin Sci (Lond)* 107: 5: 449-460, 2004.
- 537 18. **Hoeft A, Sonntag H, Stephan H and Kettler D.** Validation of myocardial oxygen demand
538 indices in patients awake and during anesthesia. *Anesthesiology* 75: 1: 49-56, 1991.
- 539 19. **Hyodo E, Hirata K, Hirose M, Sakanoue Y, Nishida Y, Arai K, Kawarabayashi T,**
540 **Shimada K, Hozumi T, Muro T, Homma S, Yoshikawa J and Yoshiyama M.** Detection of
541 restenosis after percutaneous coronary intervention in three major coronary arteries by
542 transthoracic Doppler echocardiography. *J Am Soc Echocardiogr* 23: 5: 553-559, 2010.
- 543 20. **Katz LN and Feinberg H.** The relation of cardiac effort to myocardial oxygen consumption
544 and coronary flow. *Circ Res* 6: 5: 656-669, 1958.
- 545 21. **Kazmaier S, Weyland A, Buhre W, Stephan H, Rieke H, Filoda K and Sonntag H.**
546 Effects of respiratory alkalosis and acidosis on myocardial blood flow and metabolism in
547 patients with coronary artery disease. *Anesthesiology* 89: 4: 831-837, 1998.
- 548 22. **Kobayashi Y, Fearon WF, Honda Y, Tanaka S, Pargaonkar V, Fitzgerald PJ, Lee DP,**
549 **Stefanick M, Yeung AC and Tremmel JA.** Effect of Sex Differences on Invasive Measures of
550 Coronary Microvascular Dysfunction in Patients With Angina in the Absence of Obstructive
551 Coronary Artery Disease. *JACC Cardiovasc Interv* 8: 11: 1433-1441, 2015.

- 552 23. **Krzanowski M, Bodzon W and Dimitrow PP.** Imaging of all three coronary arteries by
553 transthoracic echocardiography. An illustrated guide. *Cardiovasc Ultrasound* 1: 16, 2003.
- 554 24. **Lethen H, Tries HP, Brechtken J, Kersting S and Lambertz H.** Comparison of
555 transthoracic Doppler echocardiography to intracoronary Doppler guidewire measurements for
556 assessment of coronary flow reserve in the left anterior descending artery for detection of
557 restenosis after coronary angioplasty. *Am J Cardiol* 91: 4: 412-417, 2003.
- 558 25. **Leuenberger UA, Gray K and Herr MD.** Adenosine contributes to hypoxia-induced
559 forearm vasodilation in humans. *J Appl Physiol (1985)* 87: 6: 2218-2224, 1999.
- 560 26. **Markwalder J and Starling EH.** A note on some factors which determine the blood-flow
561 through the coronary circulation. *Am J Physiol* 47: 4-5: 275-285, 1913.
- 562 27. **Meadows GE, O'Driscoll DM, Simonds AK, Morrell MJ and Corfield DR.** Cerebral
563 blood flow response to isocapnic hypoxia during slow-wave sleep and wakefulness. *J Appl*
564 *Physiol.(1985)* 97: 4: 1343-1348, 2004.
- 565 28. **Miller MR, Hankinson J, Brusasco V, Burgos F, Casaburi R, Coates A, Crapo R,**
566 **Enright P, van der Grinten CP, Gustafsson P, Jensen R, Johnson DC, MacIntyre N,**
567 **McKay R, Navajas D, Pedersen OF, Pellegrino R, Viegi G, Wanger J and ATS/ERS Task**
568 **Force.** Standardisation of spirometry. *Eur Respir J* 26: 2: 319-338, 2005.
- 569 29. **Momen A, Mascarenhas V, Gahremanpour A, Gao Z, Moradkhan R, Kunselman A,**
570 **Boehmer JP, Sinoway LI and Leuenberger UA.** Coronary blood flow responses to
571 physiological stress in humans. *Am J Physiol Heart Circ Physiol* 296: 3: H854-861, 2009.

- 572 30. **Mosher P, Ross J,Jr, McFate PA and Shaw RF.** Control of Coronary Blood Flow by an
573 Autoregulatory Mechanism. *Circ Res* 14: 250-259, 1964.
- 574 31. **Murthy VL, Naya M, Foster CR, Hainer J, Gaber M, Di Carli G, Blankstein R, Dorbala**
575 **S, Sitek A, Pencina MJ and Di Carli MF.** Improved cardiac risk assessment with noninvasive
576 measures of coronary flow reserve. *Circulation* 124: 20: 2215-2224, 2011.
- 577 32. **Neill WA and Hattenhauer M.** Impairment of myocardial O₂ supply due to
578 hyperventilation. *Circulation* 52: 5: 854-858, 1975.
- 579 33. **Rigo F, Gherardi S, Galderisi M, Pratali L, Cortigiani L, Sicari R and Picano E.** The
580 prognostic impact of coronary flow-reserve assessed by Doppler echocardiography in non-
581 ischaemic dilated cardiomyopathy. *Eur Heart J* 27: 11: 1319-1323, 2006.
- 582 34. **Rooke T and Sparks HV.** Arterial CO₂, myocardial O₂ consumption, and coronary blood
583 flow in the dog. *Circ Res* 47: 2: 217-225, 1980.
- 584 35. **Rowe GG, Castillo CA and Crumpton CW.** Effects of hyperventilation on systemic and
585 coronary hemodynamics. *Am Heart J* 63: 67-77, 1962.
- 586 36. **Rudski LG, Lai WW, Afilalo J, Hua L, Handschumacher MD, Chandrasekaran K,**
587 **Solomon SD, Louie EK and Schiller NB.** Guidelines for the echocardiographic assessment of
588 the right heart in adults: a report from the American Society of Echocardiography endorsed by
589 the European Association of Echocardiography, a registered branch of the European Society of
590 Cardiology, and the Canadian Society of Echocardiography. *J Am Soc Echocardiogr* 23: 7: 685-
591 713; quiz 786-8, 2010.

- 592 37. **Severinghaus JW.** Simple, accurate equations for human blood O₂ dissociation
593 computations. *J Appl Physiol Respir Environ Exerc Physiol* 46: 3: 599-602, 1979.
- 594 38. **St John Sutton M, Cerkenvenik J, Borlaug BA, Daubert C, Gold MR, Ghio S, Chirinos**
595 **JA, Linde C and Ky B.** Effects of Cardiac Resynchronization Therapy on Cardiac Remodeling
596 and Contractile Function: Results From Resynchronization Reverses Remodeling in Systolic Left
597 Ventricular Dysfunction (REVERSE). *J Am Heart Assoc* 4: 9: e002054, 2015.
- 598 39. **Stembridge M, Ainslie PN, Hughes MG, Stohr EJ, Cotter JD, Tymko MM, Day TA,**
599 **Bakker A and Shave R.** Impaired myocardial function does not explain reduced left ventricular
600 filling and stroke volume at rest or during exercise at high altitude. *J Appl Physiol.*(1985) 119:
601 10: 1219-1227, 2015.
- 602 40. **Suboc TB, Strath SJ, Dharmashankar K, Harmann L, Couillard A, Malik M, Haak K,**
603 **Knabel D and Widlansky ME.** The Impact of Moderate Intensity Physical Activity on Cardiac
604 Structure and Performance in Older Sedentary Adults. *IJC Heart & Vessels* 4: 19-24, 2014.
- 605 41. **Suga H.** Total mechanical energy of a ventricle model and cardiac oxygen consumption. *Am*
606 *J Physiol.* 236: 3: H498-505, 1979.
- 607 42. **Szulik M, Sliwinska A, Lenarczyk R, Szymala M, Kalinowski ME, Markowicz-Pawlus**
608 **E, Kalarus Z and Kukulski T.** 3D and 2D left ventricular systolic function imaging-- from
609 ejection fraction to deformation. Cardiac resynchronization therapy--substudy. *Acta Cardiol* 70:
610 1: 21-30, 2015.

611 43. **Takaoka H, Takeuchi M, Otake M and Yokoyama M.** Assessment of myocardial oxygen
612 consumption (VO_2) and systolic pressure-volume area (PVA) in human hearts. *Eur Heart J* 13
613 Suppl E: 85-90, 1992.

614 44. **Tremblay JC, Lovering AT, Ainslie PN, Stembridge M, Burgess KR, Bakker A,**
615 **Donnelly J, Lucas SJ, Lewis NC, Dominelli PB, Henderson WR, Dominelli GS, Sheel AW**
616 **and Foster GE.** Hypoxia, not pulmonary vascular pressure induces blood flow through
617 intrapulmonary arteriovenous anastomoses. *J Physiol (Lond)* 593: 3: 723-737, 2014.

618 45. **Tune JD.** Control of coronary blood flow during hypoxemia. *Adv Exp Med Biol* 618: 25-39,
619 2007.

620 46. **Tune JD, Richmond KN and Gorman MW.** Control of coronary blood flow during
621 exercise. *Exp Biol Med (Maywood)* 227: 4: 238-250, 2002.

622 47. **Tymko MM, Ainslie PN, MacLeod DB, Willie CK and Foster GE.** End tidal-to-arterial
623 CO_2 and O_2 gas gradients at low- and high-altitude during dynamic end-tidal forcing. *Am J*
624 *Physiol Regul Integr Comp Physiol* 308: 11: R895-906, 2015.

625 48. **Tymko MM, Hoiland RL, Kuca T, Boulet LM, Tremblay JC, Pinske BK, Williams AM**
626 **and Foster GE.** Measuring the human ventilatory and cerebral blood flow response to CO_2 : a
627 technical consideration for the end-tidal-to-arterial gas gradient. *J Appl Physiol (1985)* 120: 2:
628 282-296, 2016.

629 49. **Tzou WS, Korcarz CE, Aeschlimann SE, Morgan BJ, Skatrud JB and Stein JH.**
630 Coronary flow velocity changes in response to hypercapnia: assessment by transthoracic Doppler
631 echocardiography. *J Am Soc Echocardiogr* 20: 4: 421-426, 2007.

632 50. **Vance JP, Brown DM and Smith G.** The effects of hypocapnia on myocardial blood flow
633 and metabolism. *Br J Anaesth* 45: 5: 455-463, 1973.

634 51. **Vantanajal JS, Ashmead JC, Anderson TJ, Hepple RT and Poulin MJ.** Differential
635 sensitivities of cerebral and brachial blood flow to hypercapnia in humans. *J Appl Physiol* (1985)
636 102: 1: 87-93, 2007.

637 52. **Venkateshvaran A, Sola S, Govind SC, Dash PK, Barooah B, Shahgaldi K, Sahlen A,**
638 **Lund L, Winter R, Nagy AI and Manouras A.** The impact of arterial load on left ventricular
639 performance: an invasive haemodynamic study in severe mitral stenosis. *Am J Physiol* 593: 8:
640 1901-1912, 2015.

641 53. **Xie A, Skatrud JB, Puleo DS and Morgan BJ.** Exposure to hypoxia produces long-lasting
642 sympathetic activation in humans. *J Appl Physiol* (1985) 91: 4: 1555-1562, 2001.

643 54. **Yang HJ, Yumul R, Tang R, Cokic I, Klein M, Kali A, Sobczyk O, Sharif B, Tang J, Bi**
644 **X, Tsaftaris SA, Li D, Conte AH, Fisher JA and Dharmakumar R.** Assessment of
645 myocardial reactivity to controlled hypercapnia with free-breathing T2-prepared cardiac blood
646 oxygen level-dependent MR imaging. *Radiology* 272: 2: 397-406, 2014.

647 55. **Yokoyama I, Inoue Y, Kinoshita T, Itoh H, Kanno I and Iida H.** Heart and brain
648 circulation and CO₂ in healthy men. *Acta Physiol* 193: 3: 303-308, 2008.

649 56. **Zhang C, Rogers PA Daphne Merkus D, Muller-Delp JM, Riefenbacher CP, Potter B,**
650 **Knudson JD, Rocic P, Chilian WM.** Regulation of coronary microvascular resistance in health
651 and disease. *Comp Physiol* 2011. Supplement 9: Handbook of Physiology, The Cardiovascular
652 System, Microcirculation: 521-549. First Published in print 2008. DOI: 10.1002/cphy.cp020412

653

654

Table 1. Cardiovascular and hemodynamic responses to hypo- and hypercapnia

	Baseline	-8 mmHg	-4 mmHg	+4 mmHg	+8 mmHg
LAD_{vmax} (cm/s)	30.6 ± 1.1	30.4 ± 1.5	31.1 ± 1.1	36.0 ± 1.9	40.7 ± 1.8 *
P_{ET}CO₂ (mmHg)	40.9 ± 1.0	33.5 ± 0.9 *	37.5 ± 0.6 *	45.3 ± 0.8 *	48.8 ± 0.8 *
P_{ET}O₂ (mmHg)	93.7 ± 1.7	92.5 ± 1.5	92.8 ± 1.9	93.9 ± 1.9	94.5 ± 2.2
SpO₂ (%)	97.2 ± 0.3	97.7 ± 0.2	97.4 ± 0.3	97.5 ± 0.3	97.2 ± 0.4
SBP (mmHg)	110 ± 4	118 ± 3	119 ± 3	125 ± 3 *	134 ± 4 *
DBP (mmHg)	59 ± 2	62 ± 2	64 ± 2	68 ± 2 *	73 ± 2 *
HR (/min)	58 ± 3	61 ± 3	57 ± 2	65 ± 3	67 ± 2
ESV (ml)	48.1 ± 3.2	48.9 ± 2.8	49.8 ± 2.9	49.5 ± 2.5	46.6 ± 2.3
EDV (ml)	109.3 ± 5.6	109.6 ± 5.1	108.9 ± 5.4	108.1 ± 5.5	108.3 ± 5.6
RPP (mmHg•beats/min)	6352 ± 391	7226 ± 467	6758 ± 345	8056 ± 457 *	8975 ± 411 *
PV_A (J)	0.63 ± 0.04	0.67 ± 0.03	0.69 ± 0.03	0.72 ± 0.04	0.77 ± 0.04

Abbreviations: LAD_{vmax}, peak diastolic velocity of the left anterior descending coronary artery; P_{ET}CO₂, end-tidal partial pressure of CO₂; P_{ET}O₂, end-tidal partial pressure of O₂; SpO₂, oxygen saturation of hemoglobin; SBP, systolic blood pressure; DBP, diastolic blood pressure; HR, heart rate; ESV, end systolic volume; EDV, end diastolic volume; RPP, rate pressure product; PV_A, energy expended by the heart in one cardiac cycle. *P<0.05, compared to baseline

Table 2. Cardiovascular and hemodynamic responses to hypoxia

	Baseline	64 mmHg	52 mmHg	45 mmHg
LAD_{Vmax} (cm/s)	29.3 ± 1.5	34.1 ± 1.2	40.6 ± 3.2*	44.9 ± 1.6*
P_{ET}CO₂ (mmHg)	40.4 ± 0.6	40.9 ± 0.7	40.5 ± 0.7	40.2 ± 0.7
P_{ET}O₂ (mmHg)	93.4 ± 1.4	64.5 ± 0.4 *	53.0 ± 0.30 *	46.3 ± 0.3 *
SpO₂ (%)	97.7 ± 0.3	92.7 ± 0.4 *	86.3 ± 0.5 *	79.9 ± 0.6 *
SBP (mmHg)	117 ± 5	127 ± 3	129 ± 3	135 ± 3 *
DBP (mmHg)	64 ± 3	70 ± 3	71 ± 3	74 ± 3
HR (/min)	55 ± 2	61 ± 2	66 ± 2 *	71 ± 3 *
ESV (ml)	47.1 ± 2.4	47.7 ± 2.7	47.2 ± 3.0	46.7 ± 2.6
EDV (ml)	106.7 ± 5.6	107.0 ± 5.9	109.3 ± 6.0	105.4 ± 5.6
RPP (mmHg•beats/min)	6505 ± 447	7801 ± 374	8469 ± 326 *	9648 ± 508 *
PV_A (J)	0.67 ± 0.04	0.74 ± 0.04	0.75 ± 0.04	0.77 ± 0.04

Abbreviations: LAD_{Vmax}, peak diastolic velocity of the left anterior descending coronary artery; P_{ET}CO₂, end-tidal partial pressure of CO₂; P_{ET}O₂, end-tidal partial pressure of O₂; SpO₂, oxygen saturation of hemoglobin; SBP, systolic blood pressure; DBP, diastolic blood pressure; HR, heart rate; ESV, end systolic volume; EDV, end diastolic volume; RPP, rate pressure product; PV_A, energy expended by the heart in one cardiac cycle. *P<0.05, compared to baseline

Figure Legends

Figure 1. Representative pulsed wave Doppler recording from the left anterior descending coronary artery. (A) Baseline Doppler waveform. (B) Doppler waveform recorded during mild hypercapnia ($P_{ET}CO_2$ = baseline + 4 mmHg)

Figure 2. Non-invasive pressure volume loop during resting conditions. Derived from Echocardiographic volume measurements and photoplethysmography blood pressure measurements. The area of the pressure volume loop represents stroke work (SW), the slope plotted tangentially to the systolic mean represents LV elastance (E_{nd}) and the area beneath it represents potential energy (PE). Data is represented as mean \pm SEM.

Figure 3. Cardiovascular and hemodynamic responses to hypo- and hypercapnia. The relationships between (A) LAD_{Vmean} , (B) mean arterial pressure (MAP), (C) coronary vascular resistance (CVR), (D) total LV mechanical energy (ME_{LV}) during the hypo- and hypercapnic trials. All values are mean \pm SEM. * $P < 0.05$, compared to baseline.

Figure 4. Coronary reactivity to hypo- and hypercapnia for individual subjects. Correlation of LAD_{Vmean} and $P_{ET}CO_2$. Dotted lines represent individual sensitivities and solid line represents mean sensitivity.

Figure 5. Cardiovascular and hemodynamic responses to hypoxia. The relationships between (A) LAD_{Vmean} , (B) mean arterial pressure (MAP), (C) coronary vascular resistance (CVR), (D) total LV mechanical energy (ME_{LV}) during the hypo- and hypercapnic trials. All values are mean \pm SEM. * $P < 0.05$, compared to baseline.

Figure 6. Coronary reactivity to hypoxia for individual subjects. Correlation of LAD_{Vmean} and $P_{ET}O_2$. Dotted lines represent individual sensitivities and solid line represents mean sensitivity.

Figure 1

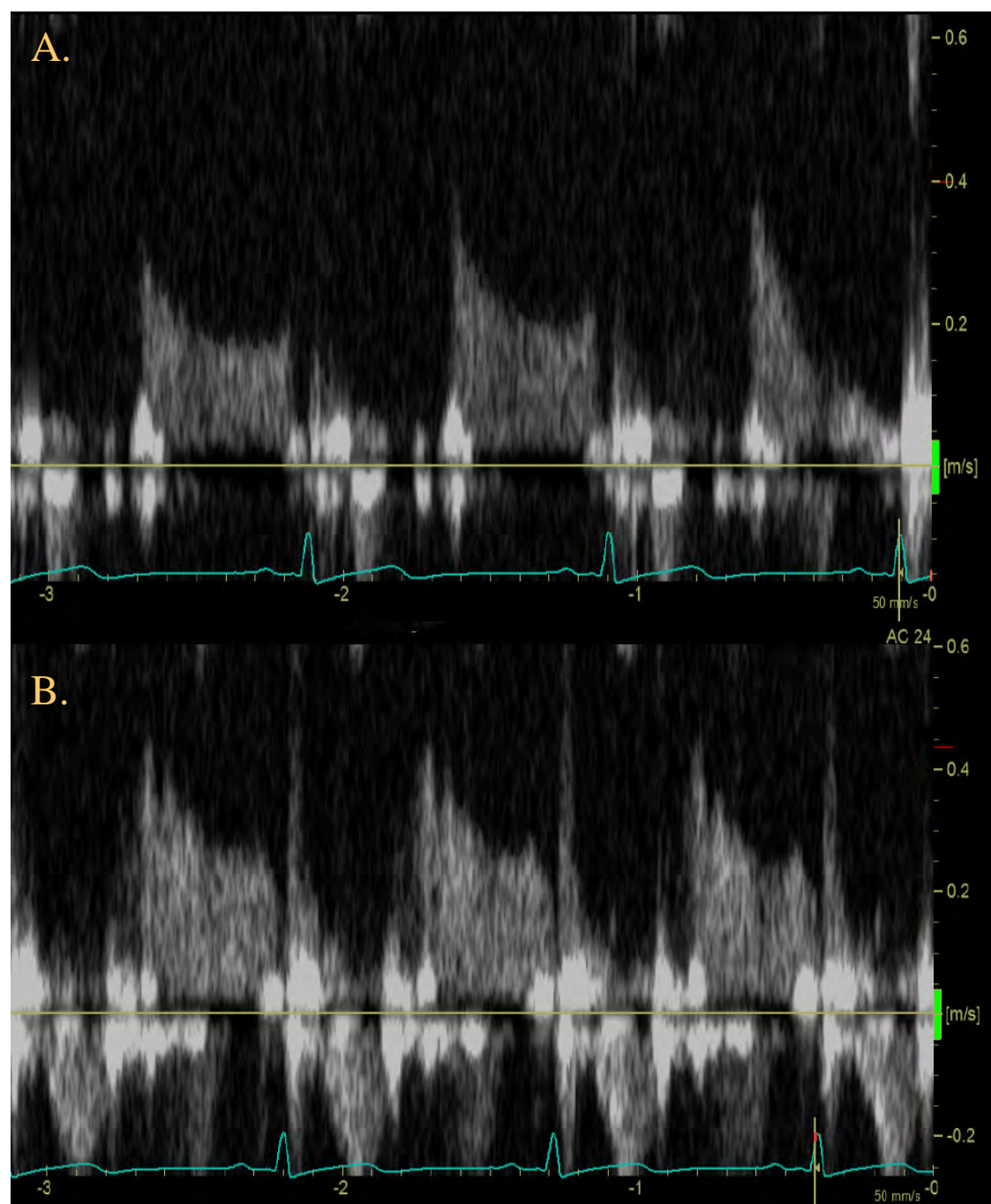


Figure 2

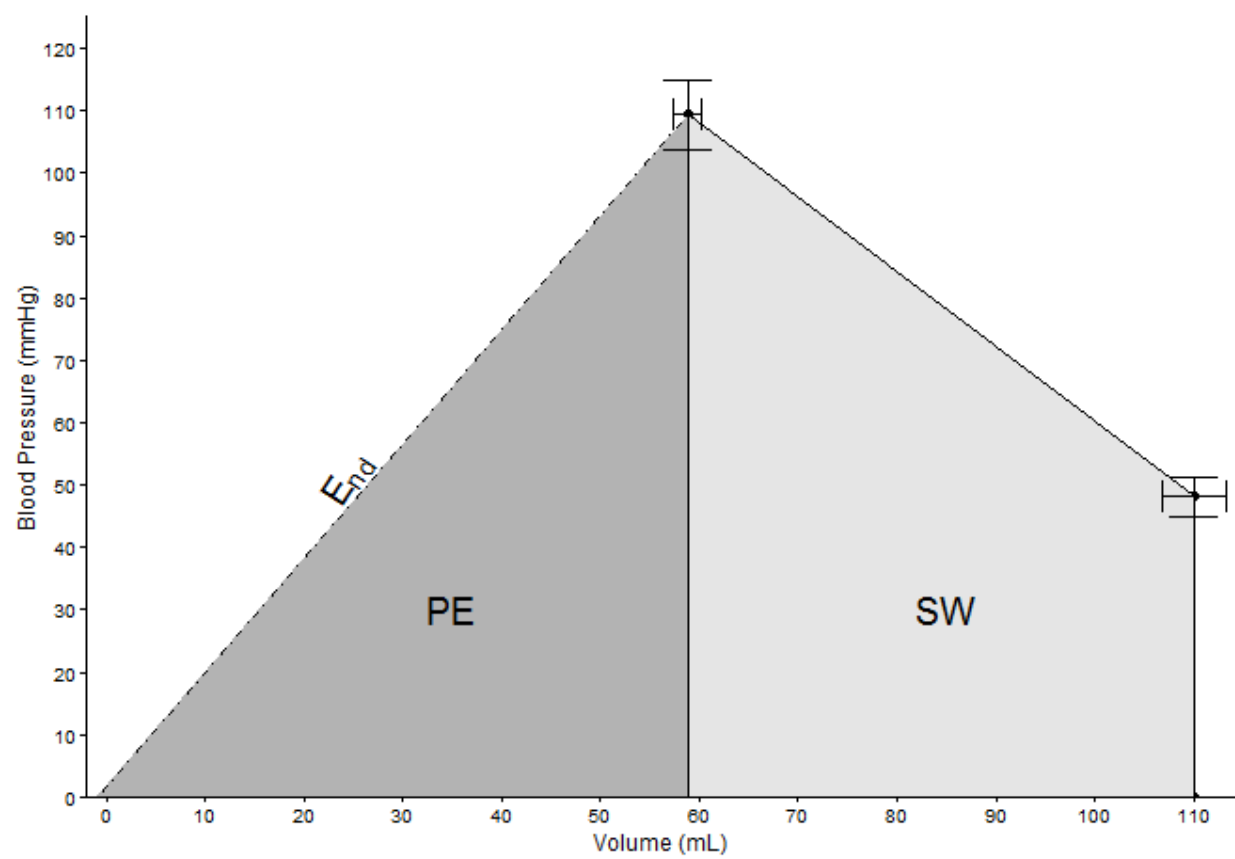


Figure 3

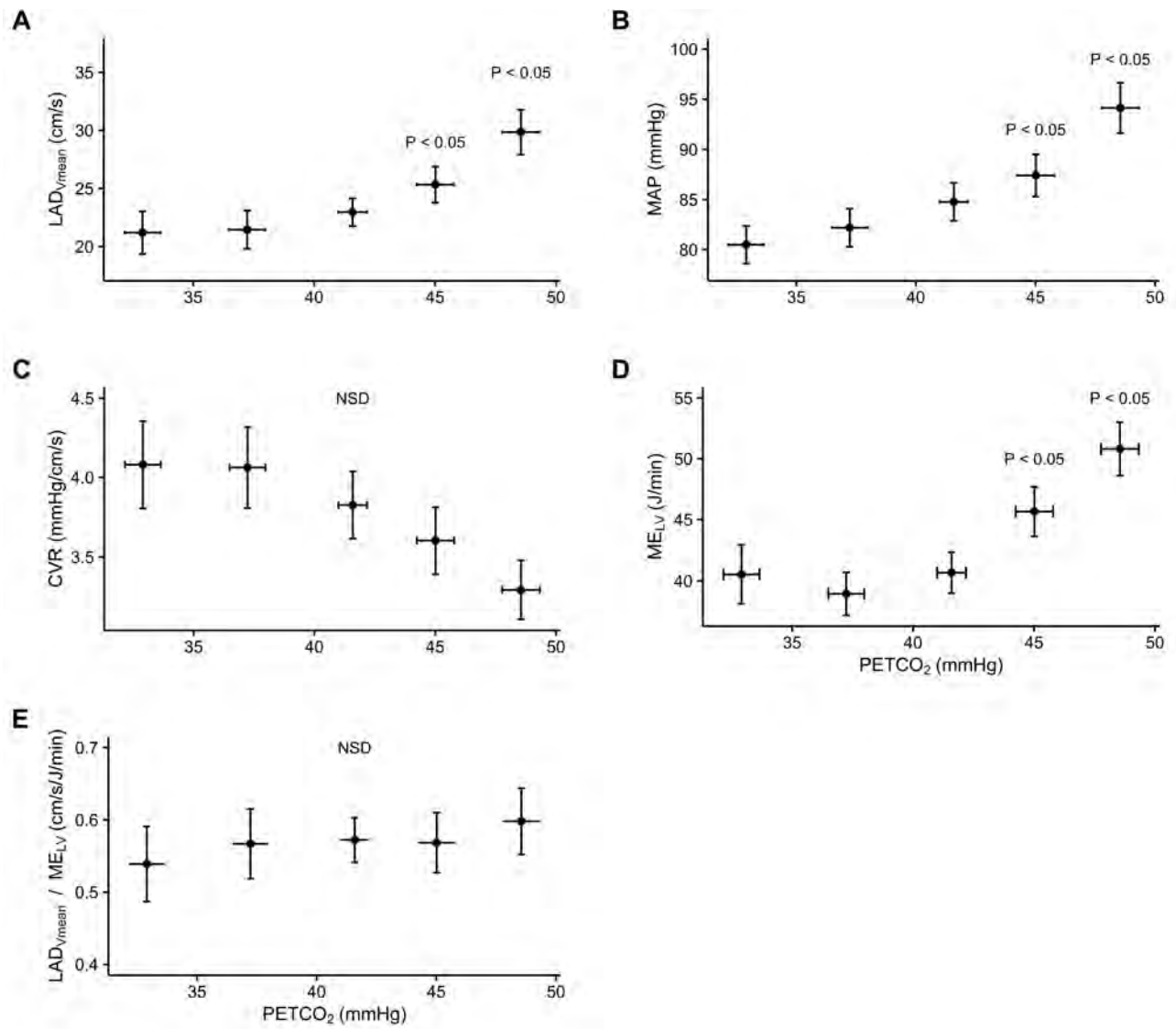


Figure 4

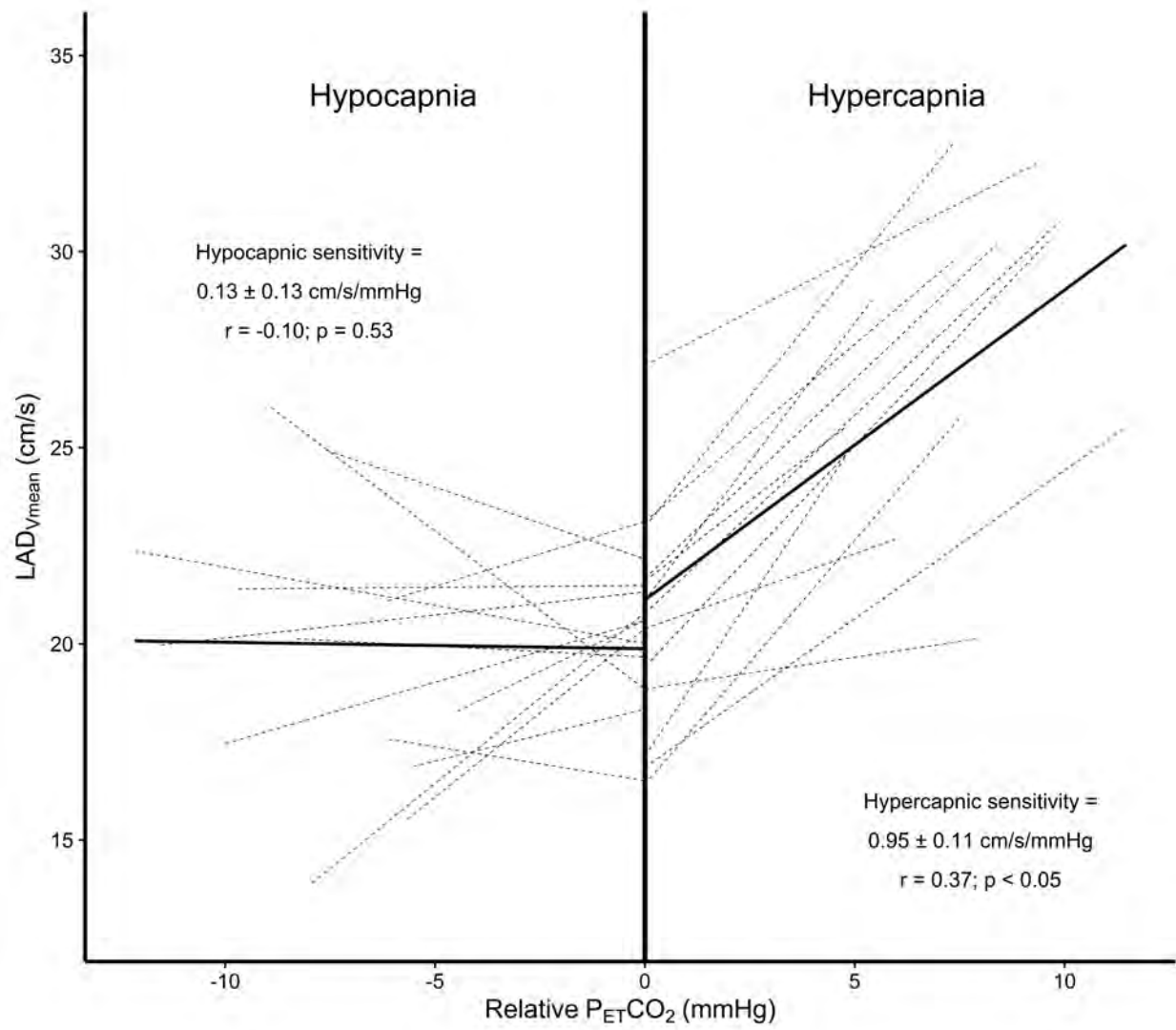


Figure 5

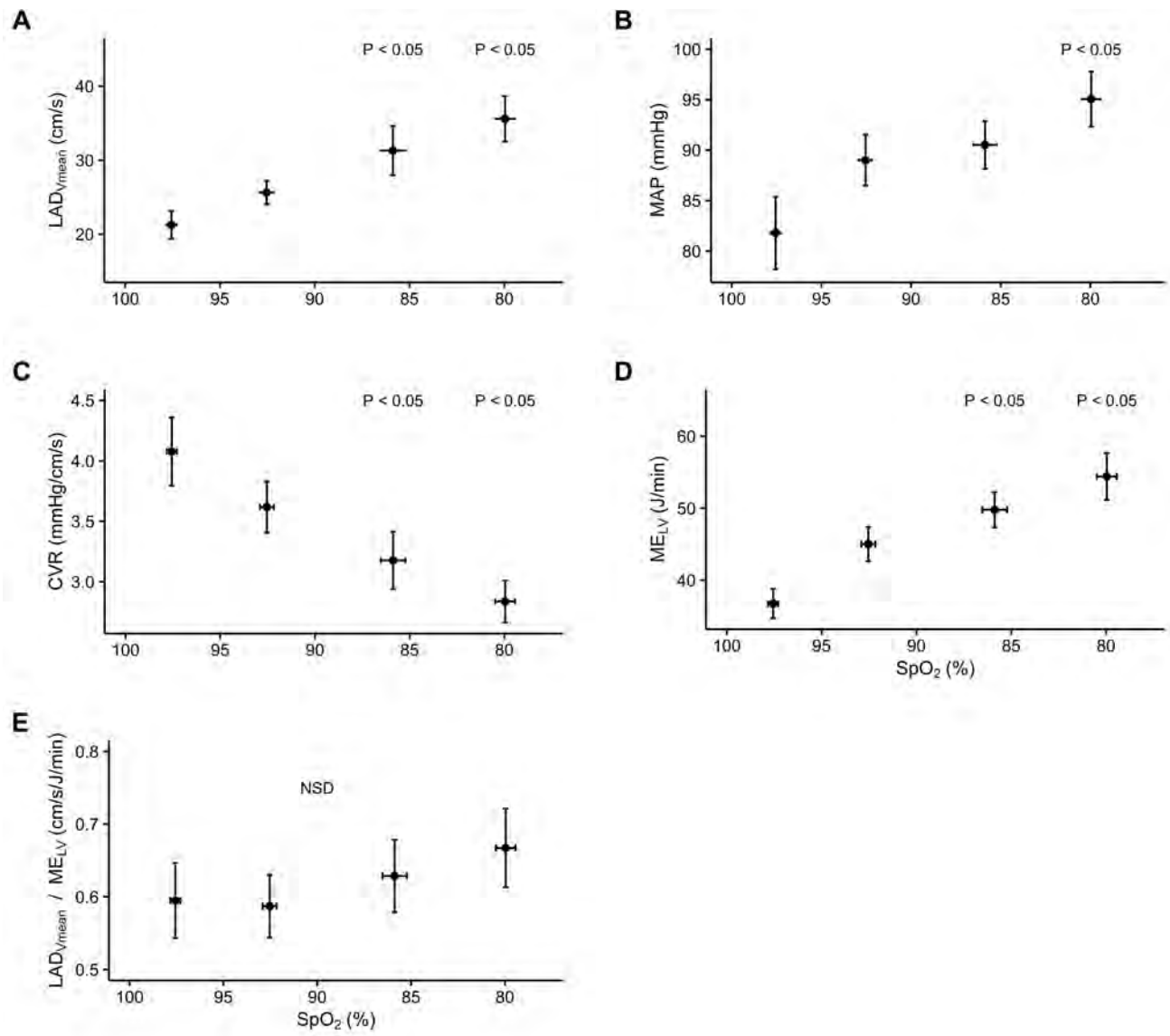


Figure 6

